

A New Bivariate Point Process Model with Application to Social Media User Content Generation

Jingfei Zhang¹ and Yongtao Guan²

^{1,2} *Department of Management Science, Miami Business School,
University of Miami, Coral Gables, FL.*

Abstract

In this paper, we propose a new bivariate point process model to study the activity patterns of social media users. The proposed model not only is flexible to accommodate but also can provide meaningful insight into the complex behaviors of modern social media users. A composite likelihood approach and a composite EM estimation procedure are developed to overcome the challenges that arise in parameter estimation. Furthermore, we show consistency and asymptotic normality of the resulting estimator. We apply our proposed method to Donald Trump's Twitter data and study if and how his tweeting behavior evolved before, during and after the presidential campaign. Moreover, we apply our method to a large-scale social media data and find interesting subgroups of users with distinct behaviors. Additionally, we discuss the effect of social ties on a user's online content generating behavior.

Keywords: point processes; composite likelihood; composite EM algorithm; social media.

1 Introduction

The use of social media has grown rapidly since the last decade, fundamentally transforming how we act, learn and interact. An important characteristic of modern social media is that a significant amount of the content consumed online is generated by users themselves (Sun and Zhu, 2013). Many prominent social media platforms rely heavily on user generated content, such as Facebook, YouTube, LinkedIn, Twitter, and Pinterest. With the growing popularity of user-contributed websites, understanding user content generating behavior becomes an increasingly important task. On one hand, it plays a crucial role in many business decisions. For example, optimizing online advertisement placement requires knowledge on how users interact with these user-contributed websites (Daugherty et al., 2008). On the other hand, understanding user content generating behavior also has important implications in social studies. For example, recent studies suggest that more connections in social networks can increase a user’s content generating activity (Ghose and Han, 2011; Sun et al., 2017).

Due to its importance, studying user content generating behavior has received much recent attention (Guo et al., 2009; Ghose and Han, 2011; Sun and Zhu, 2013; Zaman et al., 2014; Zhao et al., 2015; Fox et al., 2016; Xia et al., 2016; Sun et al., 2017). However, most existing works focus on the dissemination of information through user generated content or the factors that may affect a user’s content generating activity. The mechanism in which a user generates the content is yet to be studied and is the focus of this work. This is a difficult task as modern social media users exhibit distinct yet complex patterns in their behaviors, which consequently poses challenges in developing models that can adequately characterize the underlying processes.

Our work is motivated by two datasets collected respectively from Twitter and Sina Weibo, a popular social media site in China that is akin to a hybrid of Facebook and Twitter. The first dataset contains tweeting times from Donald Trump (@realDonaldTrump), the 45th and current President of the United States, from January 2013 to April 2018. For this dataset, we are interested in studying if and how Trump’s tweeting behavior evolved over time, in particular, before, during and after the presidential campaign. The second dataset contains posting times from a large group of Sina Weibo users in a one-month period (see Section 7.2 for more details). We are interested in characterizing the different posting behaviors among users and understanding what might have contributed to the differences. For both Twitter and Sina Weibo, a user can generate original content, which we refer to as an *original post*, or repost content from accounts that the user is following, which we refer

to as a *repost*. These two different types of content are distinguished in our datasets.

In our preliminary analysis of the two datasets, we have noticed three interesting characteristics. First, the posting times of a user are highly clustered. This observation is not entirely surprising, as it may be natural to expect a user’s interaction with social media sites to alternate between active and inactive states. During an active state, the user publishes original posts and/or reposts from others, often with a short inter-event distance; during an inactive state, the user does not generate any content or remains “offline” until the start of the next active state. As a result, the posting times appear in clusters, which we subsequently refer to as *episodes*. The second characteristic is also related to the clustering pattern of the observed events. We notice that an episode usually has alternating original post and repost clusters, i.e., a user tends to publish several consecutive original posts or reposts. We subsequently refer to these original post and repost clusters as *segments* in an episode. Third, for the Sina Weibo data, we find that certain covariates of the users can be correlated with the temporal patterns of one type of event but not the other. For example, the number of accounts a user follows is correlated (positively) with the number of reposts from the user but not the number of original posts. This indicates that original post and repost events may have different generative mechanisms and the two mechanisms are affected by different factors, such as user covariates.

A useful approach to model clustered temporal point patterns is to treat the observed posting times from a user as a realization from a clustered point process. For our two motivating datasets, since we observe two types of events, we may further view the posting times from each user as a realization from a bivariate clustered point process. Several models have been proposed for bivariate clustered point processes, the most popular of which are arguably the Hawkes process (Hawkes, 1971) and the Cox process (Cox and Lewis, 1972; Diggle and Milne, 1983). The latter includes popular models such as the log Gaussian Cox process (Møller et al., 1998) and the shot noise Cox process (Neyman and Scott, 1958; Waagepetersen, 2007) as special examples. However, neither type of processes can fully account for the user characteristics described in the previous paragraph. In particular, a bivariate Hawkes process is a mutually exciting process, and therefore, if certain covariates of the users are correlated with the temporal patterns of one type of event, then they should also be correlated with that of the other type. For the Sina Weibo data, the number of accounts that a user follows appears to be correlated with the number of reposts from the user but not with that of original posts. Thus, a bivariate Hawkes process may not be

appropriate for this dataset. Moreover, for our applications, the Hawkes process and the log Gaussian Cox process provide very limited model interpretability as neither of them is formulated in terms of clusters. As explained in the previous paragraph, a user’s interaction with social media is expected to alternate between active and inactive states (i.e., states of using and not using the social media), resulting in separated clusters (i.e., nonoverlapping episodes) of posting times. From a scientific point of view, we may wish to understand how a user transitions between active and inactive states, as well as how the user generates original posts and reposts within each event cluster. As a result, neither process can be used to answer these questions. We note that although the shot noise Cox process is formulated based on actual clusters, it may not be appropriate for our applications as the clusters in the shot noise Cox process may overlap. See Section 2 for a more detailed comparison of our proposed model with existing ones.

In this paper, we propose a new bivariate point process model. The proposed model has the flexibility to accommodate the complex characteristics observed in social media data. Specifically, our model specifies distributions for the number of segments within an episode, the number of events in each type of segment, the inter-event distance between each type of event and the time-varying distance between two adjacent episodes. As a result, the parameters in the model have straightforward interpretations and can therefore provide meaningful insights into a user’s content generating behavior. This is an important contribution of our proposed approach. For example, for a given user, such as Donald Trump, our model can estimate the user’s average length of engagement and the number of tweets generated with each Twitter usage; such insights cannot be obtained using the Hawkes process or the Cox process. Moreover, our proposed model allows the distribution of one type of event to be altered without having to change that of the other. As such, the distribution of the original post (repost) times can be altered, while that of the repost (original post) times remains unchanged. This allows, for example, covariates to be correlated with the temporal patterns of one type of events but not the other. This flexibility is especially important if one considers jointly modeling posting times from different users.

The rest of the paper is organized as follows. Section 2 presents the proposed bivariate point process model. Section 3 introduces a composite likelihood estimation approach. We describe a composite likelihood EM algorithm and show its convergence to the maximum composite likelihood estimator. Section 4 presents a procedure to assess goodness of fit. Section 5 demonstrates the effectiveness of the proposed method through simulation stud-

ies. Section 6 discusses consistency and asymptotic normality of the maximum composite likelihood estimator. We also discuss the variance-covariance matrix estimation of the parameters. Section 7 applies the proposed method to the Donald Trump’s Twitter data and the Sina Weibo user data. We discuss some practical implications of the results. Section 8 provides discussions and some concluding remarks.

2 Model Formulation

Consider the observation window $[0, T]$. The observed event locations can be written as $\{T_1, T_2, \dots, T_N\}$, where $0 \leq T_1 < T_2, \dots < T_N \leq T$ and N is a random variable taking nonnegative integer values. We assume that the events arrive in non-overlapping episodes, and each episode contains alternating *original post* and *repost* segments (see Figure 1). We refer to the first event of an episode as a *parent event* and the remaining events in an episode as *offspring events*. We assume episodes are non-overlapping since two episodes of usage are separated by an inactive or offline period for social media users; this is a unique feature of the user content generation process (Raghavan et al., 2014). Note that in our study, the temporal locations and the original post/repost labels of events are observed but not the parent/offspring labels.

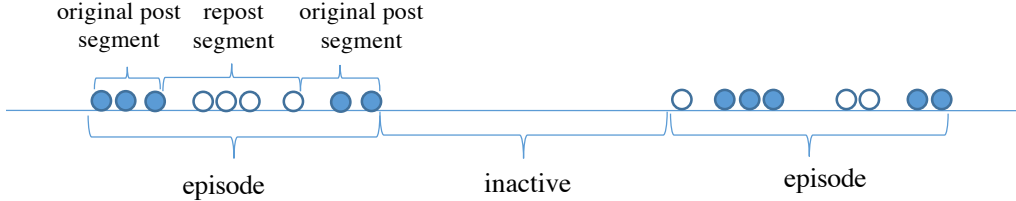


Figure 1: Illustration of episodes and segments.

Define two indicator variables X_l and Y_l , $l = 1, \dots, N$. We let $X_l = 1$ if the l -th event is an original post and $X_l = 0$ if it is a repost. Furthermore, we let $Y_l = 1$ if the l -th event is a parent event and $Y_l = 0$ otherwise. We assume that an episode starts with an original post or a repost with probabilities α or $1 - \alpha$. Moreover, we assume that the number of segments in an episode is $1 + Pois(\gamma)$, and the numbers of events in an original post and a repost segment are $1 + Pois(\mu_1)$ and $1 + Pois(\mu_0)$, respectively, where γ , μ_1 and μ_0 are all nonnegative. Poisson distributions are used here but can be replaced by other distributions generating nonnegative integers.

Let $D_l = T_l - T_{l-1}$, $l = 1, \dots, N$, be the gap times between adjacent events, where $T_0 = 0$. Let $f_{l1}(d)$, $f_{l0}^1(d)$ and $f_{l0}^0(d)$ be the probability density functions of D_l given $\{Y_l = 1\}$, $\{Y_l = 0, X_l = 1\}$ and $\{Y_l = 0, X_l = 0\}$, respectively. We assume that $f_{l1}(d)$, $f_{l0}^1(d)$ and $f_{l0}^0(d)$ are parametric functions depending on some unknown parameters $\boldsymbol{\beta}$, $\boldsymbol{\rho}_1$ and $\boldsymbol{\rho}_0$, respectively. We assume that

$$f_{l1}(d) = \lambda(t_{l-1} + d; \boldsymbol{\beta}) \exp \left[- \int_{t_{l-1}}^{t_{l-1} + d} \lambda(t; \boldsymbol{\beta}) dt \right], \quad (1)$$

where $\lambda(t; \boldsymbol{\beta})$ is a parametric hazard function for a parent event. This specification reflects that the probability of a user starting a new episode may vary with time. To avoid an overly complex model, we assume that $f_{l0}^1(d)$ and $f_{l0}^0(d)$ do not depend on the temporal location of t_l (see Section 8 for more discussions). For example, we may assume the offspring gap times follow exponential distributions, i.e.,

$$f_{l0}^1(d) = \rho_1 \exp(-\rho_1 d) \text{ and } f_{l0}^0(d) = \rho_0 \exp(-\rho_0 d), \quad (2)$$

Other distributions such as the Weibull distribution can also be used.

One important characteristic of a user's content generating behavior is its strong daily cyclic pattern (Guo et al., 2009). To capture this characteristic, we may consider an exponential sinusoidal hazard function for parent events, i.e.,

$$\lambda(t; \boldsymbol{\beta}) = \exp \left\{ \beta_{01} + \sum_{j=1}^q [\beta_{j1} \cos(\omega_j t) + \beta_{j2} \sin(\omega_j t)] \right\}, \quad (3)$$

where $\omega_j = 2j\pi$, $j = 1, \dots, q$ and $\boldsymbol{\beta} = (\beta_{01}, \beta_{11}, \beta_{12}, \dots, \beta_{q1}, \beta_{q2})^\top$. Alternatively, we can model $\lambda(t; \boldsymbol{\beta})$ as

$$\lambda(t; \boldsymbol{\beta}) = \exp \left\{ \sum_{i=1}^q \beta_i B_i(t - \lfloor t \rfloor) \right\}, \quad (4)$$

where $B_1(\cdot), \dots, B_q(\cdot)$ are q cyclic B-spline basis functions defined on $[0, 1]$ and $\boldsymbol{\beta} = (\beta_1, \dots, \beta_q)^\top$.

Under the proposed model, the expected number of offspring in an episode and the expected length of an episode are presented in the next Theorem.

Theorem 1 *In the proposed model, the expected number of offspring in an episode is*

$$\frac{1}{2}(2 + \mu_1 + \mu_0)(\gamma + 1) + c(\gamma, \alpha)(\mu_1 - \mu_0),$$

where $c(\gamma, \alpha) = e^{-\gamma}(\alpha - 1/2) \sum_{k=0}^{\infty} \gamma^{2k}/(2k)!$. Denote the expected gap times for offspring original post and repost as e_1 and e_0 , respectively. The expected length of an episode is

$$\frac{1}{2} [e_1(1 + \mu_1) + e_0(1 + \mu_0)] (\gamma + 1) + c(\gamma, \alpha) [e_1(1 + \mu_1) - e_0(1 + \mu_0)].$$

The proof is given in the Supplementary Material. When $\alpha = 1/2$, we have $c(\gamma, \alpha) = 0$, and the expected number of offspring in an episode and the expected length of an episode can be simplified to $(2 + \mu_1 + \mu_0)(\gamma + 1)/2$ and $[e_1(1 + \mu_1) + e_0(1 + \mu_0)](\gamma + 1)/2$, respectively.

We note that our model is formulated in terms of gap times. For our applications, studying the gap times allows us to understand how a user may transition between active and inactive states of using social media and how the user may generate both original posts and reposts during an active state. Another approach to construct a bivariate point process is through the intensity functions. Both the Hawkes process and the Cox process are formulated via this approach. Below we briefly compare our proposed model with these models.

Consider a bivariate Hawkes process defined on \mathbb{R} . Let $N_i(B)$ denote the number of events in $B \subset \mathbb{R}$ for the i th process and define the intensity functions $\lambda_i(t) = \lim_{\Delta_t \downarrow 0} \frac{E[N_i(t, t+\Delta_t)|H_t]}{\Delta_t}$, $i = 1, 2$, where H_t denote the entire history up to time t . The intensity functions often take the form

$$\lambda_i(t) = \mu_i + \int_0^t \nu_{ii}(t-s)N_i(ds) + \int_0^t \nu_{ij}(t-s)N_j(ds),$$

where $\mu_i \in \mathbb{R}^+$ is the background intensity, and $\nu_{ii}(\cdot)$ and $\nu_{ij}(\cdot)$ are some transfer functions, for $i, j = 1, 2$ and $i \neq j$. We can see that if $\lambda_1(t)$ depends on some covariates $\mathbf{z} \in \mathbb{R}^p$, e.g., the background intensity μ_1 is a function of \mathbf{z} , then $\lambda_2(t)$ would also depend on \mathbf{z} through $N_1(\cdot)$ in the term $\int_0^t \nu_{21}(t-s)N_1(ds)$. Consequently, a bivariate Hawkes process cannot accommodate the feature that some covariates of the user are correlated with the temporal pattern of one type of event but not the other. In comparison, our proposed model characterizes the distribution of events within each type of segments separately, and thus allows the distribution of one type of offspring events to be altered without having to change that of the other.

A bivariate Cox process is defined by a bivariate random intensity process (Λ_1, Λ_2) , where given $(\Lambda_1, \Lambda_2) = (\lambda_1, \lambda_2)$, the two component processes are independent Poisson processes with intensity functions λ_1 and λ_2 , respectively. For a log-Gaussian Cox process, we have $\Lambda_i(t) = \exp[Y_i(t)]$, $i = 1, 2$, where $\{(Y_1(t), Y_2(t)), t \in \mathbb{R}\}$ is a bivariate Gaussian process. We can see that the log Gaussian Cox process is not formulated in terms of clusters. For a shot

noise Cox process, we have $\Lambda_i(t) = \sum_{c \in \Phi_i} \eta_i k_i(t, c)$, where $\eta_i > 0$, $k_i(\cdot, \cdot)$ is a kernel, and Φ_i is a Poisson point process, $i = 1, 2$. By construction, events associated with the same parent $c \in \Phi_i$ form one cluster. It is clear that the clusters may overlap. Although it may be appropriate to have overlapping clusters in certain applications (Waagepetersen, 2007), it is more natural to view the different episodes in our applications as nonoverlapping.

3 Parameter Estimation

3.1 Likelihood function

In our study, the event locations $\mathbf{t} = \{t_1, \dots, t_n\}$ and the original post/repost labels $\mathbf{x} = \{x_1, \dots, x_n\}$ are observed. The parent/offspring labels $\mathbf{y} = \{y_1, \dots, y_n\}$ are not observed, since we do not know whether or not if an event is the first event of an episode. In our estimation approach, we treat $\mathbf{y} = \{y_1, \dots, y_n\}$ as missing data and derive the observed-data likelihood function. We assume that the first event is a parent event, i.e., $y_1 = 1$, and all events of the last episode are contained in $[0, T]$. We write the total number of episodes as K ($K = \sum_{l=1}^n y_l$), the number of segments in the k -th episode as n_k and the number of events in the j -th segment of the k -th episode as l_{kj} , $j = 1, \dots, n_k$, $k = 1, \dots, K$. Furthermore, we define an indicator z_{kj} such that $z_{kj} = 1$ if the j -th segment in the k -th episode is an original post segment and $z_{kj} = 0$ otherwise, $j = 1, \dots, n_k$, $k = 1, \dots, K$.

Write $\boldsymbol{\theta} = \{\alpha, \gamma, \mu_1, \mu_0, \boldsymbol{\rho}_1, \boldsymbol{\rho}_0, \boldsymbol{\beta}\}$. The joint density of \mathbf{t} , \mathbf{y} and \mathbf{x} for a given $\boldsymbol{\theta}$ can be written as

$$\begin{aligned} f(\mathbf{t}, \mathbf{x}, \mathbf{y} | \boldsymbol{\theta}) &= \left[\prod_{l=1}^n \sum_{h=0}^1 f_{lh}(d_l; \boldsymbol{\theta})^{I(y_l=h)} \right] P(D_{n+1} > T - t_n) \\ &\times \prod_{l=1}^n \alpha^{I(y_l=1, x_l=1)} (1 - \alpha)^{I(y_l=1, x_l=0)} \times \prod_{k=1}^K \frac{\gamma^{n_k-1} e^{-\gamma}}{(n_k - 1)!} \\ &\times \prod_{k=1}^K \prod_{j=1}^{n_k} \frac{(\mu_1^{l_{kj}-1} e^{-\mu_1})^{I(z_{kj}=1)} (\mu_0^{l_{kj}-1} e^{-\mu_0})^{I(z_{kj}=0)}}{(l_{kj} - 1)!}, \end{aligned} \quad (5)$$

where $d_l = t_l - t_{l-1}$, $l = 1, \dots, n$, and D_{n+1} is the gap time between t_n and the next parent event. With straightforward algebra, we have

$$P(D_{n+1} > T - t_n) = \exp \left[- \int_{t_n}^T \lambda(t; \boldsymbol{\beta}) dt \right].$$

Note the above density function is written as a function of gap times d_l , $l = 1, \dots, n$. The observed-data likelihood function can be written as

$$L(\boldsymbol{\theta}; \mathbf{t}, \mathbf{x}) = \sum_{\mathbf{y} \in \mathcal{Y}} f(\mathbf{t}, \mathbf{x}, \mathbf{y} | \boldsymbol{\theta}), \quad (6)$$

where \mathcal{Y} is the set of all binary vectors of length n with $y_1 = 1$. To ease the notation, when summing over all possible \mathbf{y} 's in \mathcal{Y} , we write it as $\sum_{\mathbf{y}}$ without emphasizing that $\mathbf{y} \in \mathcal{Y}$.

To estimate $\boldsymbol{\theta}$, directly maximizing the likelihood function in (6) is computationally impractical, since the number of elements in \mathcal{Y} grows exponentially with n , making the exact evaluation of the sum extremely difficult. An alternative approach is to employ an EM algorithm that treats Y_1, \dots, Y_n as missing data. However, it can be shown that the E-step in the EM procedure requires the calculation of $P_{\boldsymbol{\theta}}(Y_l = h | \mathbf{t}, \mathbf{x})$ for a given $\boldsymbol{\theta}$, $h = 0, 1$, $l = 1, \dots, n$. We have

$$P_{\boldsymbol{\theta}}(Y_l = h | \mathbf{t}, \mathbf{x}) = \frac{\sum_{\mathbf{y}|y_l=h} f(\mathbf{t}, \mathbf{x}, \mathbf{y} | \boldsymbol{\theta})}{\sum_{\mathbf{y}} f(\mathbf{t}, \mathbf{x}, \mathbf{y} | \boldsymbol{\theta})},$$

where $\mathbf{y}|y_l = h$ denotes \mathbf{y} with y_l fixed at h . Since the above expression cannot be further simplified, calculating the numerator and denominator given $y_1 = 1$ requires summing over 2^{n-2} and 2^{n-1} terms, respectively. Therefore, calculating the conditional probabilities in the E-step remains a computationally intensive task. To overcome the computational difficulty, we consider a composite likelihood approach in the next section.

3.2 Composite likelihood

The composite likelihood approach makes statistical estimation and inference through an inference function derived by multiplying a collection of component likelihoods (Lindsay, 1988). Each component is usually a conditional or marginal density, and therefore, the resulting estimating equation is unbiased (Varin et al., 2011). The composite likelihood approach has been considered for spatial point process models. For example, Guan (2006) considered a pairwise composite likelihood function. In our composite likelihood approach, instead of considering the full likelihood defined on the entire observation window $[0, T]$, we consider likelihood components defined on several equal length sub-windows. Write the length of a sub-window as $s \in \mathbb{R}$. We divide $[0, T]$ into M nonoverlapping sub-windows, i.e., $[0, T] = \bigcup_{m=1}^M [ms - s, ms)$. Define $\mathbf{t}_m = \{t_i : t_i \in [ms - s, ms), i = 1, \dots, n\}$, $m = 1, \dots, M$. We use binary vectors \mathbf{y}_m and \mathbf{x}_m to indicate the parent/offspring events and

original posts/reposts in \mathbf{t}_m , respectively.

In each sub-window, we assume that the first event is a parent event and all the events in the last episode are contained in the sub-window. Neither assumption is restrictive from a practical point of view. A typical user is inactive during some fixed time interval at night and such an interval can be identified by examining the posting times. By setting day as the sub-window, a post made right before or after that interval is therefore the last event from the previous episode or a parent event for the next episode. Under these assumptions, we can write the composite likelihood function as

$$\begin{aligned} L_s^c(\boldsymbol{\theta}; \mathbf{t}, \mathbf{x}) &= \prod_{m=1}^M f(\mathbf{t}_m, \mathbf{x}_m | \boldsymbol{\theta}) \\ &= \prod_{m=1}^M \sum_{\mathbf{y}_m} f(\mathbf{t}_m, \mathbf{y}_m, \mathbf{x}_m | \boldsymbol{\theta}), \end{aligned}$$

where $f(\mathbf{t}_m, \mathbf{x}_m | \boldsymbol{\theta}) = \sum_{\mathbf{y}_m} f(\mathbf{t}_m, \mathbf{y}_m, \mathbf{x}_m | \boldsymbol{\theta})$ and $f(\mathbf{t}_m, \mathbf{y}_m, \mathbf{x}_m | \boldsymbol{\theta})$ is defined as in (5). Hence, the log composite likelihood function can be written as

$$\ell_s^c(\boldsymbol{\theta}; \mathbf{t}, \mathbf{x}) = \sum_{m=1}^M \log \left[\sum_{\mathbf{y}_m} f(\mathbf{t}_m, \mathbf{y}_m, \mathbf{x}_m | \boldsymbol{\theta}) \right]. \quad (7)$$

Calculating $f(\mathbf{t}_m, \mathbf{x}_m | \boldsymbol{\theta}) = \sum_{\mathbf{y}_m} f(\mathbf{t}_m, \mathbf{y}_m, \mathbf{x}_m | \boldsymbol{\theta})$ requires summing over $2^{|\mathbf{y}_m|-1}$ terms, $m = 1, \dots, M$, where $|\cdot|$ denotes the number of elements in a vector or a set. When $\sup_m |\mathbf{y}_m| \ll |\mathbf{y}|$, the calculation can be performed much more efficiently. Moreover, the computation cost $O(\sum_{m=1}^M 2^{|\mathbf{y}_m|})$ only increases approximately linearly with the observation window length $T = Ms$. It is worth mentioning that if we can identify several events as parent events a priori, the computational complexity can be further reduced. We present the computational details in the Supplementary Material.

To find the maximum composite likelihood estimator $\hat{\boldsymbol{\theta}}_{M,s}$, a straightforward approach is to directly maximize the log composite likelihood function in (7) using numerical methods. However, this can be problematic in instances where the log composite likelihood function in (7) has a flat surface. In such cases, the numerical methods may take a long time to converge. Moreover, both the computation time and the convergence result can be sensitive to the starting values. If the starting values are not chosen carefully, the numerical maximization methods may even fail to converge. The numerical difficulty with maximizing the log

composite likelihood becomes more severe when more parameters are included in the model. A similar observation was also made in Veen and Schoenberg (2008), who investigated the flatness of the log likelihood function of the Hawkes process and the limitations of using numerical methods to find the maximum likelihood estimator (MLE).

Additionally, in the numerical maximization methods, each step needs to maximize

$$\ell_s^c(\boldsymbol{\theta}; \mathbf{t}, \mathbf{x}) = \sum_{m=1}^M \log \left[\sum_{\mathbf{y}_m} f(\mathbf{t}_m, \mathbf{y}_m, \mathbf{x}_m | \boldsymbol{\theta}) \right]$$

with respect to the high-dimensional parameter vector $\boldsymbol{\theta} = (\alpha, \gamma, \mu_1, \mu_0, \boldsymbol{\rho}_1, \boldsymbol{\rho}_0, \boldsymbol{\beta})$ with constraints such as $0 < \alpha < 1$, $\gamma, \mu_1, \mu_0 > 0$. This maximization is very computationally intensive.

To overcome these challenges in parameter estimation, we describe a composite likelihood EM estimation procedure in the next section.

3.3 Composite likelihood EM algorithm

The EM procedure is a useful approach for finding the MLE with missing data (Dempster et al., 1977). The algorithm iterates between an E-step, in which the expected log likelihood of the complete data is computed conditional on the observed data, and an M-step, in which the expected log likelihood from the E-step is maximized to update the parameters.

Applying the standard EM algorithm to find the maximum composite likelihood estimator requires calculating $\mathbf{y} | \mathbf{t}, \mathbf{x}$ for a given $\boldsymbol{\theta}$. Evaluating this conditional distribution directly is computationally impractical (see discussion in Section 3.1). To overcome this challenge, we use a composite likelihood EM algorithm that only requires calculating $\mathbf{y}_m | \mathbf{t}_m, \mathbf{x}_m$, $m = 1, \dots, M$, for a given $\boldsymbol{\theta}$. To that end, define

$$Q(\boldsymbol{\theta} | \boldsymbol{\theta}_{p-1}) = \sum_{m=1}^M E_{\mathbf{Y}_m | \mathbf{t}_m, \mathbf{x}_m, \boldsymbol{\theta}_{p-1}} \log [f(\mathbf{t}_m, \mathbf{Y}_m, \mathbf{x}_m | \boldsymbol{\theta})],$$

where $\boldsymbol{\theta}_{p-1}$ is the updated parameter after completing the $(p-1)$ -th iteration of the composite likelihood EM algorithm.

The composite likelihood EM algorithm iterates between the following E-step and M-step until convergence.

- E-step: Given the previous update $\boldsymbol{\theta}_{p-1}$, obtain $Q(\boldsymbol{\theta} | \boldsymbol{\theta}_{p-1})$.

- M-step: Maximize $Q(\boldsymbol{\theta}|\boldsymbol{\theta}_{p-1})$ with respect to $\boldsymbol{\theta}$ to produce an updated $\boldsymbol{\theta}_p$.

To justify the composite likelihood EM algorithm, we establish the following ascent property.

Theorem 2 *The composite log-likelihood $\ell_s^c(\boldsymbol{\theta}; \mathbf{t}, \mathbf{x})$ and the composite likelihood EM sequence $\boldsymbol{\theta}_p$ satisfy*

$$\ell_s^c(\boldsymbol{\theta}_p; \mathbf{t}, \mathbf{x}) \geq \ell_s^c(\boldsymbol{\theta}_{p-1}; \mathbf{t}, \mathbf{x}),$$

where the equality holds if and only if $Q(\boldsymbol{\theta}_p|\boldsymbol{\theta}_{p-1}) = Q(\boldsymbol{\theta}_{p-1}|\boldsymbol{\theta}_{p-1})$, $p = 1, 2, \dots$

See the Supplementary Material for proof. Theorem 2 guarantees that the log composite likelihood is non-decreasing at each EM iteration. Since $Q(\boldsymbol{\theta}|\boldsymbol{\theta}')$ is continuous in both $\boldsymbol{\theta}$ and $\boldsymbol{\theta}'$, the converge of $\boldsymbol{\theta}_p$ to a stationary point as $p \rightarrow \infty$ is guaranteed by Theorem 2 in Wu (1983). Since the convergence is only guaranteed to a stationary point, common techniques such as running the EM algorithm from multiple starting points can help locate the global maximum.

Computational details on the optimization in the M-step of the composite likelihood EM algorithm can be found in the Supplementary Material. We consider both exponential and Weibull distributions for offspring gap times. Most parameter updates have closed-form expressions. Hence the M-step in the EM procedure can be achieved efficiently. While we do not observe notable differences in the parameters estimated from the EM algorithm and the numerical maximization methods (in the cases that they do converge) in our simulation studies, numerical methods on average take at least 15 times longer to reach convergence.

4 Goodness of Fit

Having estimated the parameters in the proposed model, it is important to assess whether the estimated model fits the point patterns observed in the data. Residual analysis as a goodness of fit assessment has been considered by others (see for example Baddeley et al., 2005). However, such analysis cannot be applied to our setting since the intensity function of our model is difficult to derive. Alternatively, we evaluate the goodness of fit by checking whether the fitted model can adequately capture the inhomogeneity in the gap times calculated from the observed data. To accomplish this, we compare the empirical distribution function of the observed gap times to that calculated from realizations simulated from the fitted model.

The gap time distribution function from the observed data, denoted as $\hat{F}(v)$, is calculated as:

$$\hat{F}(v) = \frac{1}{n} \sum_{l=1}^n I(d_l < v),$$

where $d_l = t_l - t_{l-1}$, $l = 1, \dots, n$. We can calculate the distribution functions denoted as $\hat{F}^{(i)}(v)$, $i = 1, \dots, w$, from w independent realizations in $[0, T]$ from the fitted model. Define

$$\begin{aligned} \bar{F}(v) &= \frac{1}{w} \sum_{i=1}^w \hat{F}^{(i)}(v), \\ U(v) &= \max\{\hat{F}^{(i)}(v)\}, \\ L(v) &= \min\{\hat{F}^{(i)}(v)\}. \end{aligned}$$

To evaluate the goodness of fit, we plot $\hat{F}(v)$ against $\bar{F}(v)$ along with the upper and lower simulation envelopes $U(v)$ and $L(v)$. If the fitted model is compatible with the observed data, the plot of $\hat{F}(v)$ against $\bar{F}(v)$ should be roughly linear and contained in the simulation envelopes.

We may wish to further investigate the gap time distributions for offspring original posts, offspring reposts and parent posts. Denote the gap times for the offspring original posts and reposts by E_1 and E_0 , respectively. Define $F_i(v) = P(E_i < v)$, $i = 0, 1$. From the estimated model, both $F_1(v)$ and $F_0(v)$ can be easily calculated. For example, if we assume an exponential distribution for E_1 , then $F_1(v) = 1 - \exp(-\hat{\rho}_1 v)$. Furthermore, we can estimate $F_1(v)$ with

$$\hat{F}_1(v) = \frac{\sum_{l=1}^n \pi_{l0}(\hat{\boldsymbol{\theta}}_{M,s}) I(x_l = 1) I(d_l < v)}{\sum_{l=1}^n \pi_{l0}(\hat{\boldsymbol{\theta}}_{M,s}) I(x_l = 1)}, \quad (8)$$

where $\pi_{l0}(\hat{\boldsymbol{\theta}}_{M,s}) = P(Y_l = 0 | \mathbf{t}_m, \mathbf{x}_m, \hat{\boldsymbol{\theta}}_{M,s})$, $t_l \in [ms - s, s]$ and $\hat{\boldsymbol{\theta}}_{M,s}$ is the estimate of $\boldsymbol{\theta}$ from the proposed composite likelihood EM algorithm. To assess the goodness of fit, we can compare $\hat{F}_1(v)$ to $F_1(v)$ over a range of different v values. If the assumed gap time distribution fits the data well, then $\hat{F}_1(v)$ should be close to $F_1(v)$. The goodness of fit for offspring reposts can be evaluated similarly by comparing $\hat{F}_0(v)$ against $F_0(v)$, where $\hat{F}_0(v)$ can be calculated analogous to (8).

To assess the goodness of fit for the parent event gap time distribution, we use the following result. Assume we observe event time locations at $0 = u_0 < u_1 < u_2 < \dots < u_n <$

T . Let the gap times $u_l - u_{l-1}$, $l = 1, \dots, n$, follow the density function in (1). Define

$$\Lambda(u_l) = \int_{u_{l-1}}^{u_l} \lambda(u) du, \quad l = 1, \dots, n.$$

Then, $\Lambda(u_l)$'s follow an exponential distribution with the unit rate. This is a special case of the time change theorem from Meyer (1971). Thus, we can rescale the inhomogeneous parent gap times as random variables from an exponential distribution with the unit rate. Define

$$\hat{F}_2(v) = \frac{\sum_{l=1}^n \pi_{l1}(\hat{\boldsymbol{\theta}}_{M,s}) I \left[\int_{t_{l-1}}^{t_l} \lambda(t, \hat{\boldsymbol{\beta}}) dt < v \right]}{\sum_{l=1}^n \pi_{l1}(\hat{\boldsymbol{\theta}}_{M,s})}.$$

If the estimated parent gap time distribution fits the observed pattern well, $\hat{F}_2(v)$ should be close to $F_2(v) = P(E_2 < v)$, where $E_2 \sim \exp(1)$. To assess the goodness of fit, we can compare $\hat{F}_2(v)$ to $F_2(v)$ over a range of different v values.

5 Simulation Study

In this section, we perform a simulation study to investigate the finite sample performance of the proposed method. For this purpose, we simulate point processes from the proposed model with gap time distributions given in (1) and (2) with

$$\lambda(t; \boldsymbol{\beta}) = \exp [\beta_{01} + \beta_{11} \cos(2\pi t) + \beta_{12} \sin(2\pi t)] \quad (9)$$

and $\boldsymbol{\beta} = (\beta_{01}, \beta_{11}, \beta_{12})^\top$. To simulate data from the model, we use the thinning technique proposed in Lewis and Shedler (1979). We set the observation window length $T = 100$, $\alpha = 0.6$, $\gamma = 0.5$ or 1 , $\mu_1 = 0.5$ or 1 , $\mu_0 = 0.5$ or 1 , $(\rho_1, \rho_0) = (10, 15)$ or $(20, 30)$ and $\boldsymbol{\beta}^\top = (-2, -2, 2)$ or $(-3, -3, 3)$. With each parameter configuration, we simulate 100 event trajectories.

For estimation, we use sub-window length $s = 1$ or 5 . We also considered $s = 10, 15, 20$. The results for $s = 10, 15, 20$ are not presented, since the parameter estimates are very similar to those for $s = 5$. Furthermore, to model $\lambda(t, \boldsymbol{\beta})$, we consider both the true model in (9) and the nonparametric cyclic B-spline model in (4). For the latter, we use the knot vector $(0, 0.2, 0.4, 0.6, 0.8, 1)$.

Table 1 and Table 2 show the parameter and standard error estimates when $\lambda(t, \boldsymbol{\beta})$ is

$(\gamma, \mu_1, \mu_0, \rho_1, \rho_0)$ $(\beta_{01}, \beta_{11}, \beta_{12}; s)$	α	γ	μ_1	μ_0	ρ_1	ρ_0	β_{01}	β_{11}	β_{12}
$(0.5, 0.5, 0.5, 10, 15)$ $(-2, -2, 2; 5)$	0.607 (0.007)	0.512 (0.014)	0.514 (0.014)	0.505 (0.014)	10.162 (0.217)	15.090 (0.367)	-2.086 (0.049)	-1.988 (0.042)	2.073 (0.047)
$(0.5, 0.5, 0.5, 10, 15)$ $(-3, -3, 3; 5)$	0.605 (0.007)	0.496 (0.011)	0.507 (0.013)	0.509 (0.013)	10.097 (0.179)	15.034 (0.333)	-2.899 (0.080)	-2.913 (0.057)	2.993 (0.072)
$(1.0, 0.5, 0.5, 10, 15)$ $(-2, -2, 2; 5)$	0.592 (0.007)	1.001 (0.017)	0.501 (0.011)	0.509 (0.011)	9.994 (0.196)	15.496 (0.316)	-2.067 (0.054)	-2.048 (0.045)	2.031 (0.049)
$(0.5, 1.0, 1.0, 10, 15)$ $(-2, -2, 2; 5)$	0.605 (0.007)	0.501 (0.013)	0.987 (0.019)	1.006 (0.020)	10.089 (0.154)	15.308 (0.253)	-2.055 (0.052)	-1.957 (0.048)	2.096 (0.047)
$(0.5, 0.5, 0.5, 20, 30)$ $(-2, -2, 2; 5)$	0.599 (0.007)	0.511 (0.012)	0.500 (0.013)	0.506 (0.013)	20.003 (0.543)	29.794 (0.627)	-2.136 (0.045)	-2.116 (0.041)	2.107 (0.045)
$(0.5, 0.5, 0.5, 10, 15)$ $(-2, -2, 2; 1)$	0.598 (0.007)	0.456 (0.012)	0.466 (0.012)	0.484 (0.013)	10.769 (0.217)	16.810 (0.407)	-2.013 (0.053)	-2.051 (0.042)	2.020 (0.053)

Table 1: Parameter estimation using (9) for $\lambda(t, \boldsymbol{\beta})$, with processes simulated under $\alpha = 0.6$ and different $(\gamma, \mu_1, \mu_0, \rho_1, \rho_0, \boldsymbol{\beta})$. The estimated standard errors are given in parentheses.

$(\gamma, \mu_1, \mu_0, \rho_1, \rho_0)$ $(\beta_{01}, \beta_{11}, \beta_{12}; s)$	α	γ	μ_1	μ_0	ρ_1	ρ_0
$(0.5, 0.5, 0.5, 10, 15)$ $(-2, -2, 2; 5)$	0.595 (0.010)	0.498 (0.013)	0.489 (0.014)	0.494 (0.014)	10.172 (0.261)	15.604 (0.365)
$(0.5, 0.5, 0.5, 10, 15)$ $(-3, -3, 3; 5)$	0.594 (0.007)	0.496 (0.011)	0.510 (0.012)	0.518 (0.014)	9.867 (0.188)	15.422 (0.284)
$(1.0, 0.5, 0.5, 10, 15)$ $(-2, -2, 2; 5)$	0.603 (0.009)	0.993 (0.017)	0.489 (0.011)	0.499 (0.012)	10.012 (0.176)	15.026 (0.257)
$(0.5, 1.0, 1.0, 10, 15)$ $(-2, -2, 2; 5)$	0.598 (0.008)	0.511 (0.010)	0.990 (0.016)	1.025 (0.017)	10.149 (0.171)	15.084 (0.309)
$(0.5, 0.5, 0.5, 20, 30)$ $(-2, -2, 2; 5)$	0.600 (0.008)	0.508 (0.012)	0.499 (0.012)	0.488 (0.013)	19.855 (0.460)	30.354 (0.717)
$(0.5, 0.5, 0.5, 10, 15)$ $(-2, -2, 2; 1)$	0.601 (0.008)	0.468 (0.010)	0.495 (0.014)	0.460 (0.014)	10.795 (0.271)	16.335 (0.309)

Table 2: Parameter estimation using (4) for $\lambda(t, \boldsymbol{\beta})$, with processes simulated under $\alpha = 0.6$ and different $(\gamma, \mu_1, \mu_0, \rho_1, \rho_0, \boldsymbol{\beta})$. The estimated standard errors are given in parentheses.

specified as in (9) and (4), respectively. In both tables, the estimated parameters are close to the true values when $s = 5$. With all other parameters fixed, models with $\boldsymbol{\beta}^\top = (-3, -3, 3)$ generate more episodes and segments compared to models with $\boldsymbol{\beta}^\top = (-2, -2, 2)$. Therefore, parameters γ , μ_1 , μ_0 , ρ_1 and ρ_0 are estimated better when $\boldsymbol{\beta}^\top = (-3, -3, 3)$. This can be observed by comparing the standard errors in the first and second settings in Table 1 (or Table 2). With all other parameters fixed, greater γ leads to longer episodes with more

offspring and, therefore, better estimations of μ_1 , μ_0 , ρ_1 and ρ_0 . We can observe this by comparing the standard errors in the first and the third settings in Table 1 (or Table 2). Similarly, with all other parameters fixed, greater μ_1 and μ_0 lead to longer segments with more offspring and, therefore, better estimations of ρ_1 and ρ_0 . This can be seen by comparing the standard errors in the first and fourth settings in Table 1 (or Table 2). In both of the aforementioned cases, the estimation of β suffers, since there are fewer parent events due to the decreased number of episodes within our observation window. This can be seen by comparing the standard errors for $\hat{\beta}$ in the first, third and fourth settings in Table 1. Furthermore, with all other parameters fixed, greater ρ_1 and ρ_0 lead to shorter segments and episodes; therefore, more segments and episodes are generated within the observation window, which results in better estimations of γ , μ_1 , μ_0 and β . This can be observed by comparing the standard errors in the first and the fifth settings in Table 1 (or Table 2).

From the parameter estimates in the last setting in Table 1 (or Table 2), we can see some bias when $s = 1$. However, when the sub-window length is increased to 5, we see no evidence of bias, and the estimated parameters are close to the true values. When the sub-window length is further increased, we see no noticeable difference in the results. This finding is consistent with our theoretical results.

Comparing the estimates of $\gamma, \mu_1, \mu_0, \rho_1, \rho_0$ in Table 1 and Table 2, we can see that estimating $\lambda(t, \beta)$ using B-splines gives satisfactory performance even though the true underlying hazard function is exponential sinusoidal.

6 Asymptotic Properties of $\hat{\theta}_{M,s}$

In the following theoretical development, we use θ_0 to denote the true parameter vector and Θ to denote the parameter space for θ , and we assume that Θ is compact. Consider the log composite likelihood function in (7). Its composite score function can be written as

$$U_{M,s}(\theta) = \frac{1}{sM} \sum_{m=1}^M U_{m,s}(\theta),$$

where

$$U_{m,s}(\theta) = \frac{f^{(1)}(\mathbf{t}_m, \mathbf{x}_m | \theta)}{f(\mathbf{t}_m, \mathbf{x}_m | \theta)}$$

and $f^{(1)}(\mathbf{t}_m, \mathbf{x}_m | \boldsymbol{\theta})$ is the first-order derivative with respect to $\boldsymbol{\theta}$. The maximum composite likelihood estimator $\hat{\boldsymbol{\theta}}_{M,s}$ in our proposed method is the solution to $U_{M,s}(\boldsymbol{\theta}) = 0$. Here, we write $U_{M,s}$ to signify that this score function is also a function of the sub-window length s . In the next theorem, we establish consistency of $\hat{\boldsymbol{\theta}}_{M,s}$.

Theorem 3 *Assume that the following conditions are satisfied,*

$$(2.1) \ E[U_{M,s}(\boldsymbol{\theta})] = 0 \text{ only at } \boldsymbol{\theta} = \boldsymbol{\theta}_s^*,$$

$$(2.2) \ \text{There exists a nonnegative function } \kappa(\cdot) \text{ such that}$$

$$\left| \frac{f^{(1)}(\mathbf{t}_m, \mathbf{x}_m | \boldsymbol{\theta})}{f(\mathbf{t}_m, \mathbf{x}_m | \boldsymbol{\theta})} \right| < \kappa(|\mathbf{t}_m|), \quad \left| \frac{f^{(2)}(\mathbf{t}_m, \mathbf{x}_m | \boldsymbol{\theta})}{f(\mathbf{t}_m, \mathbf{x}_m | \boldsymbol{\theta})} \right| < \kappa(|\mathbf{t}_m|),$$

and $E[\kappa(|\mathbf{t}_m|)^2] < \infty$. Here, $|\mathbf{t}_m|$ is the number of events in the m -th sub-window.

Then, $\hat{\boldsymbol{\theta}}_{M,s}$ converges in probability to $\boldsymbol{\theta}_s^*$ as $M \rightarrow \infty$. Moreover, if $E[U_{M,s}(\boldsymbol{\theta})] \rightarrow 0$ as $s \rightarrow \infty$ only at $\boldsymbol{\theta} = \boldsymbol{\theta}_0$, we have $\boldsymbol{\theta}_s^* \rightarrow \boldsymbol{\theta}_0$ as $s \rightarrow \infty$.

The proof is given in the Supplementary Material. In the theorem, we first show that $\hat{\boldsymbol{\theta}}_{M,s}$ converges to $\boldsymbol{\theta}_s^*$ as the number of sub-windows tends to infinity. If the assumptions that the first event in a sub-window is a parent event and all events of the last episode are contained in the sub-window are satisfied, we have $\boldsymbol{\theta}_s^* = \boldsymbol{\theta}_0$. Note these assumptions involve only the first and the last episodes in the window. Thus, even when these assumptions do not hold, $\boldsymbol{\theta}_s^*$ converges to $\boldsymbol{\theta}_0$ as the length of the sub-window increases. In the next lemma, we show that the model specifications considered in our work satisfy Conditions (2.1) and (2.2).

Lemma 1 *In our proposed model, when offspring gap times follow exponential distributions or Weibull distributions and the parent hazard function $\lambda(t, \boldsymbol{\beta})$ satisfies*

$$\max_j \left| \frac{\partial \lambda(t, \boldsymbol{\beta}) / \partial \beta_j}{\lambda(t, \boldsymbol{\beta})} \right| < \infty,$$

we have that Conditions (2.1) and (2.2) in Theorem 3 are satisfied. Consequently, the consistency result in Theorem 3 applies to our composite likelihood estimator.

See the Supplementary Material for proof. Next, we discuss the asymptotic normality of $\hat{\boldsymbol{\theta}}_{M,s}$ as $M \rightarrow \infty$. Following Bolthausen (1982), we first define the following mixing coefficients to quantify the dependence in the proposed point process.

Let \mathbb{N} denote the set of all natural numbers. For $\Lambda \subseteq \mathbb{N}$, let $\mathcal{F}(\Lambda)$ denote the σ -algebra generated by $U_{m,s}(\boldsymbol{\theta}_s^*)$, $m \in \Lambda$. Let $d(\Lambda_1, \Lambda_2) = \inf\{|m_1 - m_2| : m_1 \in \Lambda_1, m_2 \in \Lambda_2\}$. For all $v \in \mathbb{N}$ and $k, l \in \mathbb{N} \cup \{\infty\}$, define the following mixing coefficient:

$$\alpha_{k,l}(v) = \sup\{|P(A_1 \cap A_2) - P(A_1)P(A_2)| : A_i \in \mathcal{F}(\Lambda_i), |\Lambda_1| \leq k, |\Lambda_2| \leq l, d(\Lambda_1, \Lambda_2) \geq v\}.$$

Theorem 4 *Assume that $\sum_{v=1}^{\infty} \alpha_{k,l}(v) < \infty$ for $k + l \leq 4$, $\alpha_{1,\infty}(v) = o(v^{-1})$ and that for some $\delta > 0$, $E[(U_{m,s}(\boldsymbol{\theta}_s^*))^{2+\delta}] < \infty$ and $\sum_{v=1}^{\infty} \alpha_{1,1}(v)^{\delta/(2+\delta)} < \infty$. Define*

$$\mathcal{I}_0 = \left\{ E \left[\frac{\partial}{\partial \boldsymbol{\theta}} U_{M,s}(\boldsymbol{\theta}) \right] \right\} \Big|_{\boldsymbol{\theta}=\boldsymbol{\theta}_s^*}$$

and

$$\mathcal{I}_M^{-1} = (\mathcal{I}_0^{-1}) \left\{ \frac{1}{s^2 M} \sum_{i=1}^M \sum_{j=1}^M E \left[(U_{i,s}(\boldsymbol{\theta}_s^*) U_{j,s}^T(\boldsymbol{\theta}_s^*)) \right] \right\} (\mathcal{I}_0^{-1})^T.$$

If \mathcal{I}_M is positive definite, then $\sqrt{M}(\hat{\boldsymbol{\theta}}_{M,s} - \boldsymbol{\theta}_s^*)$ converges in distribution to $N(\mathbf{0}, \mathcal{I}_M^{-1})$.

The above result follows from Bolthausen (1982). Thus we omit the proof here. The conditions require that the dependence between two score components $U_{m_1,s}(\boldsymbol{\theta}_s^*)$ and $U_{m_2,s}(\boldsymbol{\theta}_s^*)$ decreases as $|m_1 - m_2|$ increases and the score function has bounded moments.

In practice, the variance covariance matrix \mathcal{I}_M^{-1} needs to be estimated. If we assume that the $U_{m,s}(\boldsymbol{\theta})$'s are independent, we can estimate \mathcal{I}_0 and \mathcal{I}_M^{-1} using

$$\hat{\mathcal{I}}_0 = \left[\frac{1}{sM} \sum_{i=1}^M \frac{\partial}{\partial \boldsymbol{\theta}} U_{m,s}(\boldsymbol{\theta}) \right] \Big|_{\boldsymbol{\theta}=\hat{\boldsymbol{\theta}}_{M,s}}$$

and

$$\hat{\mathcal{I}}_M^{-1} = (\hat{\mathcal{I}}_0^{-1}) \left\{ \frac{1}{s^2 M} \sum_{m=1}^M \left[U_{m,s}(\hat{\boldsymbol{\theta}}_{M,s}) U_{m,s}^T(\hat{\boldsymbol{\theta}}_{M,s}) \right] \right\} (\hat{\mathcal{I}}_0^{-1})^T,$$

where $U_{m,s}(\hat{\boldsymbol{\theta}}_{M,s})$ and $\frac{\partial}{\partial \boldsymbol{\theta}} U_{m,s}(\boldsymbol{\theta})|_{\boldsymbol{\theta}=\hat{\boldsymbol{\theta}}_{M,s}}$, $m = 1, \dots, M$, can be estimated in the last step of the composite likelihood EM procedure. Without the independence assumption on the $U_{m,s}(\boldsymbol{\theta})$'s, we can adopt a simulation approach. If we obtain parameter estimates $\boldsymbol{\theta}_1^*, \dots, \boldsymbol{\theta}_w^*$ from w realizations simulated from the model with parameter $\hat{\boldsymbol{\theta}}_{M,s}$, then \mathcal{I}_M^{-1} can be estimated using the sample covariance matrix of $\boldsymbol{\theta}_1^*, \dots, \boldsymbol{\theta}_w^*$.

7 Social Media Data Analysis

In this section, we apply our proposed model to the two datasets described in Section 1. In the first application, we study Twitter data collected from Donald Trump from January 2013 to April 2018, and characterize changes in various aspects of his tweeting behavior, such as the tweeting rate, length of each tweeting episode and daily activity level, before, during and after the presidential campaign. In the second application, we apply our proposed method to a large-scale user data collected from Sina Weibo. Through investigating different aspects of user behaviors, we find interesting user subgroups. Furthermore, we discuss the effect of social ties on a user’s posting behavior.

7.1 Donald Trump Twitter Data

In this section, we study the Twitter data collected from Donald Trump’s twitter account @realDonaldTrump. This account was opened in March 2009 and an archive of all tweets published from this account can be downloaded at <http://www.trumptwitterarchive.com/>. We focus on the time period from January 2013 to April 2018. During this period, a total of 26,493 tweets were posted from Trump’s Twitter account. Some of these tweets were posted by Trump himself while others were posted by his staff. The author of a tweet may be identified using the platform that the tweet was sent from (Auxier and Golbeck, 2017; Ott, 2017). While Trump’s staff primarily posted from computers, Trump himself posted from an Android device prior to the presidency. As president, he switched to an iPhone due to security reasons. Hence, we study the tweets made from Android before the election and from iPhone after the election and treat them as being made by Trump. This results in a total of 17,518 tweets. The average number of monthly tweets is 278 with a standard deviation of 154.

To investigate the dynamics in Trump’s tweeting behavior over time, we fit the proposed bivariate point process model to the tweets collected within each month in the study window. We model the offspring gap times using exponential distributions given in (2), and the parent hazard function using cyclic B-spline basis as in (4) with 7 equally spaced knots in $[0, 1]$, i.e., one day. We consider a sub-window with length $s = 7$ days. The estimated parameters are shown in Figure 2, in which two important months are marked. The first one is June 2015, the month in which Trump announced his candidacy for president; the second one is January 2017, the month in which he had the inauguration and assumed office.

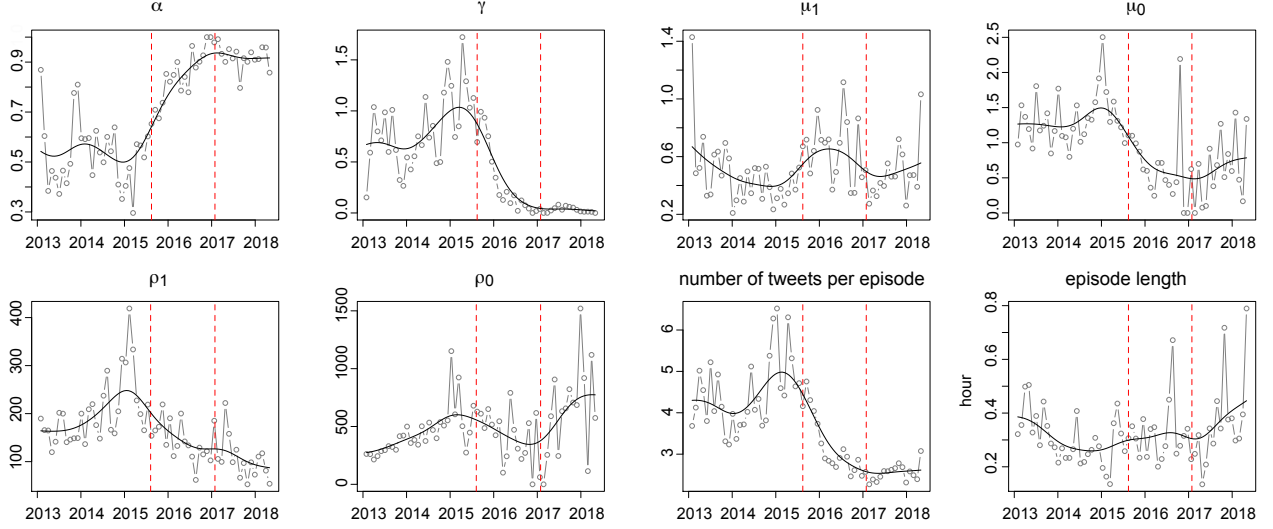


Figure 2: Parameters estimated from Donald Trump’s monthly Twitter data. The plotted points show estimated parameters for each month and the black solid lines show the Gaussian kernel smoothed curves. The two red dashed lines mark June 2015 (candidacy announcement) and January 2017 (assumed office), respectively.

From Figure 2, we can see that the tweeting behavior of Donald Trump exhibits noticeable changes over time. From the estimated α values, we can see that Trump started an episode about equally likely with either an original tweet or a retweet before the announcement of his candidacy, increasingly likely with an original tweet during the presidential campaign, and almost always with an original tweet since the presidency. There is a steady drop in the estimated γ values during the campaign, indicating fewer and fewer switches back and forth between original tweet and retweet segments within each episode. The estimated γ values are almost zero since Trump assumed office, which suggests that he typically published only one type of tweets in each episode. The estimated μ_1 values do not show strong systematic differences over time, suggesting that the number of original tweets per original tweet segment remained relatively constant over time. However, there is a decreasing trend in the estimated μ_0 values during the presidential campaign. This suggests that Trump tended to publish fewer and fewer retweets per retweet segment as the campaign continued.

The original tweet and retweet rates, i.e., ρ_1 and ρ_0 , indicate how fast a user makes an original tweet and a retweet, respectively. A larger ρ_1 (or ρ_0) value indicates a higher original tweet (or retweet) rate. The estimated ρ_1 values decrease since the start of the campaign, suggesting that Trump spent increasingly more time on writing each original tweet. On the other hand, the estimated ρ_0 values have a noticeable increase since he assumed office,

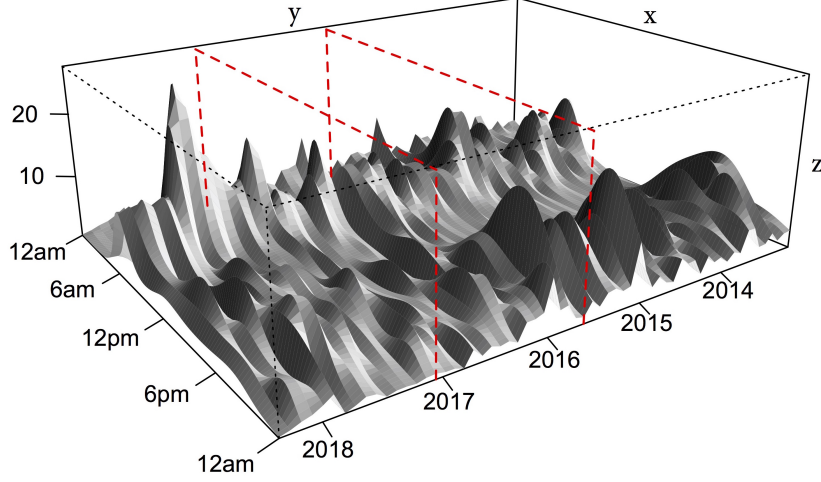


Figure 3: Estimated parent hazard functions from Donald Trump’s monthly Twitter data. The x -axis shows the time within a day, the y -axis shows the month and the z -axis shows the hazard function value. The two red dashed lines mark June 2015 (candidacy announcement) and January 2017 (assumed office), respectively.

suggesting that he retweeted much faster after he became the president.

Based on the above estimated model parameters, we estimate the number of tweets per episode and the episode length using results from Theorem 1. The estimates are shown in the last two plots of the bottom panel in Figure 2. The plot of the estimated number of tweets per episode resembles that of the estimated γ values. Before Trump announced his candidacy, he posted on average 4-5 tweets per episode. The number steadily dropped during the campaign and eventually stabilized at around 2.5 since he assumed office. The plot of the episode length shows that Trump typically spent around 15-30 minutes every time he used Twitter and the length of engagement per episode remained relatively constant over time. It is worth noting that even though there were fewer tweets per episode since the presidency, the length of an episode was not noticeably affected. This is likely attributed to the fact that he had mostly original tweets in each episode since the presidency and original tweets took more time to compose.

Figure 3 shows the estimated time-varying parent hazard function, which describes how likely Trump was to start using Twitter at any given time of the day. We can see that the activity level was consistently high in the morning around 6am-7am. The morning activity level seemed to have increased slightly since the presidency. The activity level in the afternoon had a noticeable decrease since the start of the campaign in June 2015. Before the campaign, there was a higher activity level in the afternoon with active periods concentrated

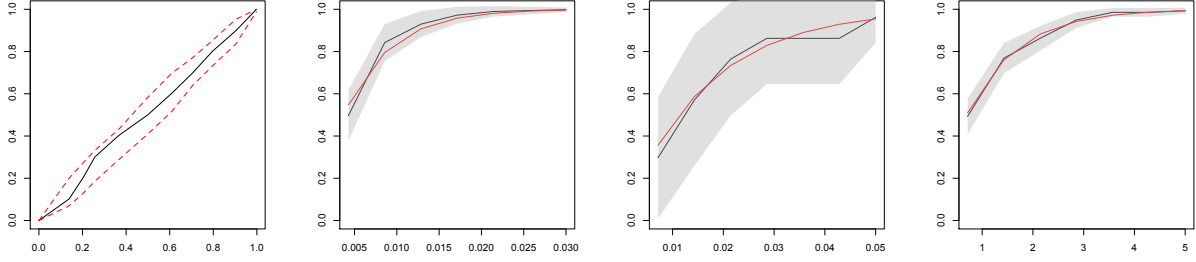


Figure 4: Goodness of fit plots of the model fitted for January 2017. From left to right are the envelop plot with the upper and lower envelopes marked in red dashed lines, goodness of fit plots for the offspring original post, offspring repost and parent inter-event distances. The red solid lines in the last three plots are calculated from cdfs of the fitted exponential distributions. The grey bands are the 95% confidence intervals.

mostly around 8pm-9pm.

To investigate the goodness of fit, we consider the procedures discussed in Section 4 for each model fitted using the monthly Twitter data. The goodness of fit plots generally suggest that our proposed model fits the data well. Figure 4 shows these plots for the model fitted for January 2017, the first month of Trump’s presidency. For the envelope plot, we simulate 99 realizations from the fitted model. We can see that the $\hat{F}(v)$ against $\bar{F}(v)$ line is roughly linear and contained in the simulation envelope. This suggests that the simulated gap times match the observed ones. Furthermore, we compare $\hat{F}_i(v)$ against $F_i(v)$, $i = 0, 1, 2$, in the last three plots of Figure 4. For the confidence intervals, the standard error of $\hat{F}_i(v)$ for a given v is approximated by assuming that distributions of gap times D_l , $l = 1, \dots, N$ are independent in the calculation. We can see that the estimated gap time distributions (i.e., $\hat{F}_i(v)$ ’s) appear to be in close agreement with their theoretical counterparts (i.e., $F_i(v)$ ’s) from the fitted model. We also consider Weibull distributions to model the offspring gap times. We do not present the results here as the fitted models are very similar (see discussion in Section 8).

7.2 Sina Weibo data analysis

Sina Weibo is one of the most popular social media sites in China. Similar to Twitter, a Sina Weibo user can follow other users and can either publish original content or repost content from other accounts. The Sina Weibo data focus on followers of the official Weibo account of a top degree program in China. Restricted by the site’s API policy, 5,918 of the following

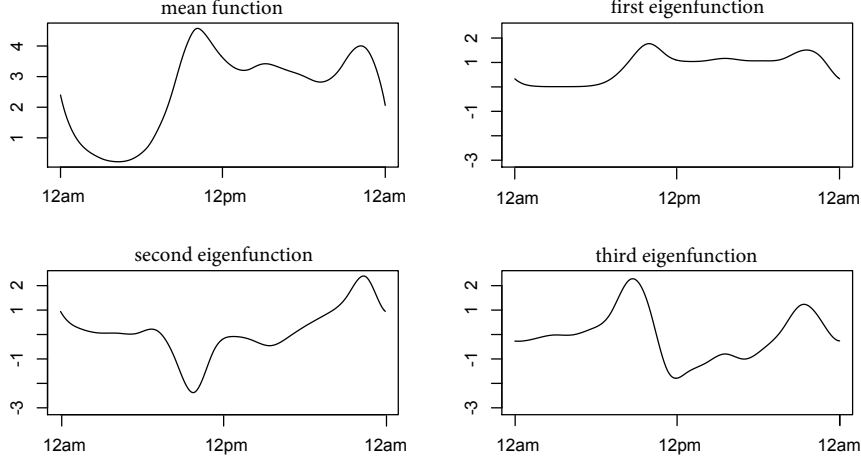


Figure 5: The mean function and the first three eigenfunctions in the functional principal component analysis of the parent hazard functions.

accounts (approximately 10% of the total) were able to be sampled. For each user, all of his/her posts during the period of January 1st-30th, 2014 were collected.

Similar to Twitter, many users on Sina Weibo are inactive users, i.e., users who do not (or very infrequently) create any content. In our study, we focus on the sampled followers who had at least 30 posts in our 30-day observation window. This subset of the sample contains 1,714 subjects. To investigate the user content generating behavior, we fit the proposed bivariate point process model to each of the 1,714 subjects. We model the offspring gap times using the exponential distributions given in (2) and the parent hazard function using cyclic B-spline basis as in (4) with 7 equally spaced knots in $[0, 1]$, i.e., one day. Furthermore, we consider a sub-window with length $s = 7$ days. To investigate the goodness of fit, we apply again the procedures discussed in Section 4 for the model fitted to each user’s data. The goodness of fit plots generally suggest that our proposed model fits the data well and we therefore omit the details.

7.2.1 Characterize Sina Weibo user behavior

The fitted model for each Sina Weibo user offers insight into the content generating behavior of the user from different aspects. To be more specific, the fitted parent hazard function describes how likely a user is to start using Sina Weibo at any given time of the day, while the fitted offspring distributions characterize the posting patterns that a user follows once he/she starts using Sina Weibo.

Given the fitted parent hazard functions from the 1,714 users, we use functional principal

component analysis to investigate the dominant modes of variation. Figure 5 shows the mean function and the first three eigenfunctions from the analysis. One notable pattern in the mean function is the extremely low activity level from 1am to 6am. This is expected as most users would be resting during this time. Two high activity levels appear around 9am-10am and 10pm-11pm. The first eigenfunction characterizes activeness from 8am to 12am with two moderate peaks around 10am and 10pm. The second eigenfunction describes contrasting activeness at around 10am and 10pm. This indicates that some users only had one activity peak at either 10am or 10pm. Similarly, the third eigenfunction suggests that some users were active in the morning (around 10am) and at night (around 10pm) but inactive during the time in between, while others were most active around noon but inactive in the morning and at night. These three eigenfunctions explain 76.61% of the total variation.

Using the parameter estimates, we further investigate the following three measurements of each user: (i) the average daily parent hazard function, which indicates how often a user uses Weibo; (ii) the expected number of posts per episode, which measures the activity level once a user starts using Weibo; (iii) the expected length of an episode, which measures the length of engagement once a user starts using Weibo. Figure 6 shows the user groups in each of the three measurements. The number of groups and the group membership are identified using gap statistics and K-means clustering. For each measure, there are high, medium and low groups, with the low groups containing the most users.

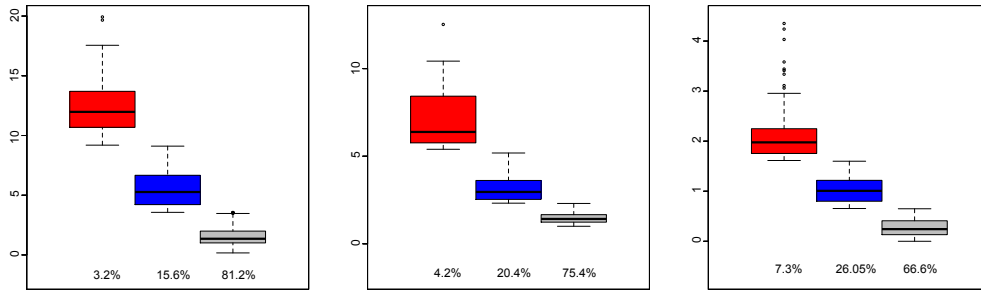


Figure 6: Groups in the average daily parent hazard (left plot), average number of posts per episode (middle plot) and average length (in hours) of an episode (right plot). The percentages at the bottom of the boxplots show the percentage of users in each group.

For the average daily parent hazard function, users in the low, medium and high groups had average hazards of 1.5, 5.6 and 12.7, respectively. For the expected number of posts per episode, users in the low, medium and high groups had, on average, 1.5, 3.1 and 7.5 posts per

episode. Considering the expected length of an episode, users in the low, medium and high groups had episodes that lasted, on average, 16 minutes, 1 hour and 2 hours, respectively.

7.2.2 Social effect on users of Sina Weibo

For each Sina Weibo user, we also have the number of accounts the user was following, which we denote as n_{\rightarrow} , and the number of accounts that were following this user, which we denote as n_{\leftarrow} . The values for n_{\leftarrow} are extremely skewed, ranging from 5 to 82 million (the values for n_{\rightarrow} only range from 0 to 3000); therefore, we consider $\log(n_{\leftarrow})$ in our analysis. In the following discussion, the standard error estimation provided after “ \pm ” is calculated using bootstrap with 10,000 replications.

In our analysis, we find that there is a moderate correlation between n_{\rightarrow} and γ ($r = 0.108 \pm 0.031$) and a stronger correlation between n_{\rightarrow} and μ_0 ($r = 0.205 \pm 0.035$). These observations indicate that users who followed many accounts tended to have more reposts. One explanation could be that the more accounts a user follows, the more content they can repost from. Another plausible explanation is that the “followers” in the social media tend to repost more. We do not see notable correlations between n_{\rightarrow} and the other estimated parameters.

Furthermore, we find that the correlation between $\log(n_{\leftarrow})$ and α is 0.218 ± 0.023 and the correlation between $\log(n_{\leftarrow})$ and μ_1 is 0.127 ± 0.026 . These observations suggest that the “popular” users, i.e., those who had many followers, tended to post more original content. They were also more likely to initiate their Weibo engagement by posting original content. We do not see notable correlations between $\log(n_{\leftarrow})$ and the other estimated parameters.

The correlation between the average daily parent hazard and $\log(n_{\leftarrow})$ is 0.242 ± 0.022 , and the correlation between the average daily parent hazard and n_{\rightarrow} is 0.159 ± 0.026 . These show that users who had strong social ties, i.e., who had many followers or followed many others, tended to use Sina Weibo more often. Lastly, the correlation between the expected length of an episode and $\log(n_{\leftarrow})$ is 0.240 ± 0.026 . This interesting observation indicates that users with many followers tended to spend more time on Sina Weibo once they started an episode of engagement.

8 Discussion

In this paper, we propose a new bivariate point process model. The proposed model offers a good balance between model complexity and model flexibility, and is highly interpretable. We develop a composite likelihood estimation approach to estimate the parameters. To improve computational efficiency and numerical stability, we adopt a composite likelihood EM estimation procedure. We discuss procedures for goodness of fit assessments. Furthermore, we show consistency and asymptotic normality of the maximum composite likelihood estimator.

We note that in applications where there is only one type of events, the proposed bivariate model can be easily modified to accommodate such univariate scenario. In this case, each episode would contain only one type of events and the alternating segments within each episode no longer need to be considered. In the model specification, we may set $\alpha = 1$, $\gamma = 0$, $\mu_0=0$ and $\rho_0=0$ and estimate only μ_1 , ρ_1 and β . This univariate model can be considered as a special case of the proposed bivariate model.

In our real data analysis, we have also used Weibull distributions to model offspring gap times. In such cases, estimates of the parameters α , γ , μ_1 , μ_0 and β remain very similar, and we do not see notable improvement in the fit of the model. For this reason, we focus on exponential offspring gap time distributions in our real data analysis.

Under our proposed modeling framework, we may consider more complex model formulations, and here we discuss a few possibilities. When fitting the proposed model to Sina Weibo user data, we assume that the gap time distributions of both offspring original posts and reposts do not vary with the time of day t . A more sophisticated model can assume that these two probability densities are functions of t . Similarly, we may also assume that γ , μ_1 and μ_0 are functions of t . Such models can capture the potentially time-varying offspring generating behavior throughout the day. We note that this would considerably increase the number of parameters in our model and consequently make the estimation more challenging. To balance complexity and flexibility, such models are not further pursued in the current paper. Considering Donald Trump’s Twitter data, we are interested in investigating changes in his tweeting behavior before, during and after the presidential campaign. To this end, we fit our proposed model to data collected for each month within the study period. Another approach could be, for example, to consider a varying coefficient model, in which we assume that α , γ , μ_1 , μ_0 , ρ_1 , ρ_0 , β are functions of day; we may fit the model using kernel smoothing technique. This would be an interesting topic to consider for future research.

References

- Auxier, B., and Golbeck, J. (2017) The president on Twitter: A characterization study of @realDonaldTrump. *International Conference on Social Informatics*, 377-390.
- Baddeley, A., Turner, R., Møller, J., and Hazelton, M. (2005) Residual analysis for spatial point processes (with discussion). *Journal of the Royal Statistical Society: Series B*, **67(5)**, 617-666.
- Bolthausen, E. (1982) On the central limit theorem for stationary mixing random fields. *The Annals of Probability*, **10(4)**, 1047-1050.
- Cox, D. R., and Lewis, P. A. W. (1972) Multivariate point processes. *Proceedings of the Sixth Berkeley Symposium on Mathematical Statistics and Probability*, **3**, 401-448.
- Crowder, M. (1986) On consistency and inconsistency of estimating equations. *Econometric Theory*, **2(3)**, 305-330.
- Daugherty, T., Eastin, M. S., and Bright, L. (2008) Exploring consumer motivations for creating user-generated content. *Journal of Interactive Advertising*, **8(2)**, 16-25.
- Dempster, A. P., Laird, N. M., and Rubin, D. B. (1977) Maximum likelihood from incomplete data via the EM algorithm. *Journal of the Royal Statistical Society. Series B*, **39(1)**, 1-38.
- Diggle, P. J., and Milne, R. K. (1983) Bivariate Cox processes: some models for bivariate spatial point patterns. *Journal of the Royal Statistical Society. Series B*, **45(1)**, 11-21.
- Fox, E. W., Short, M. B., Schoenberg, F. P., Coronges, K. D., and Bertozzi, A. L. (2016) Modeling e-mail networks and inferring leadership using self-exciting point processes. *Journal of the American Statistical Association*, **111(514)**, 564-584.
- Ghose, A., and Han, S. P. (2011) An empirical analysis of user content generation and usage behavior on the mobile Internet. *Management Science*, **57(9)**, 1671-1691.
- Guan, Y. (2006) A composite likelihood approach in fitting spatial point process models. *Journal of the American Statistical Association*, **101(476)**, 1502-1512.
- Guo, L., Tan, E., Chen, S., Zhang, X., and Zhao, Y. E. (2009) Analyzing patterns of user content generation in online social networks. *Proceedings of the 15th ACM SIGKDD International Conference on Knowledge Discovery and Data Mining*, 369-378.
- Hawkes, A. G. (1971) Spectra of some self-exciting and mutually exciting point processes. *Biometrika*, **58(1)**, 83-90.

- Lewis, P. A., and Shedler, G. S. (1979) Simulation of nonhomogeneous Poisson processes by thinning. *Naval Research Logistics Quarterly*, **26(3)**, 403-413.
- Lindsay, B. G. (1988) Composite likelihood methods. *Contemporary Mathematics*, **80**, 221-239.
- Meyer, P. A. (1971) Démonstration simplifiée d'un théorème de Knight. *Séminaire de probabilités v université de strasbourg*. Springer, Berlin, Heidelberg.
- Møller, J., Syversveen, A. R., and Waagepetersen, R. P. (1998) Log Gaussian Cox Processes. *Scandinavian Journal of Statistics*, **25(3)**, 451-482.
- Neyman, J., and Scott, E. (1958) Statistical approach to problems of cosmology. *Journal of the Royal Statistical Society, Series B*, **20**, 1-43.
- Ott, B. L. (2017). The age of Twitter: Donald J. Trump and the politics of debasement. *Critical Studies in Media Communication*, **34(1)**, 59-68.
- Raghavan, V., Ver Steeg, G., Galstyan, A., and Tartakovsky, A. G. (2014) Modeling temporal activity patterns in dynamic social networks. *IEEE Transactions on Computational Social Systems*, **1(1)**, 89-107.
- Sun, M., and Zhu, F. (2013) Ad revenue and content commercialization: evidence from blogs. *Management Science*, **59(10)**, 2314-2331.
- Sun, Y., Dong, X., and McIntyre, S. (2017) Motivation of user-generated content: social connectedness moderates the effects of monetary rewards. *Marketing Science*, in press.
- Varin, C., Reid, N., and Firth, D. (2011) An overview of composite likelihood methods. *Statistica Sinica*, **21(1)**, 5-42.
- Veen, A., and Schoenberg, F. P. (2008) Estimation of space-time branching process models in seismology using an em-type algorithm. *Journal of the American Statistical Association*, **103(482)**, 614-624.
- Xia, D., Mankad, S., and Michailidis, G. (2016) Measuring influence of users in twitter ecosystems using a counting process modeling framework. *Technometrics*, **58(3)**, 360-370.
- Waagepetersen, R. P. (2007) An estimating function approach to inference for inhomogeneous Neyman Scott processes. *Biometrics*, **63(1)**, 252-258.
- Wu, C. J. (1983) On the convergence properties of the EM algorithm. *The Annals of Statistics*, **11(1)**, 95-103.

- Zaman, T., Fox, E. B., and Bradlow, E. T. (2014). A Bayesian approach for predicting the popularity of tweets. *The Annals of Applied Statistics*, **8(3)**, 1583-1611.
- Zhao, Q., Erdogdu, M. A., He, H. Y., Rajaraman, A., and Leskovec, J. (2015) Seismic: A self-exciting point process model for predicting tweet popularity. *Proceedings of the 21th ACM SIGKDD International Conference on Knowledge Discovery and Data Mining*, 1513-1522.